Identification and characterization of protein phosphatase 2C activation by ceramide[S]

David M. Perry,* **Kazuyuki Kitatani,†** **Patrick Roddy,*** **Mohamad El-Osta,***
and Yusuf A. Hannun[1],§

Department of Biochemistry and Molecular Biology,* Medical University of South Carolina, Charleston, SC 29425; Department of Clinical Laboratory,† Tottori University Hospital, 36-1 Nishi-Cho, Yonago City, Tottori 683-8504, Japan; and Stony Brook Cancer Center,§ Stony Brook University Health Science Center, Stony Brook, NY 11794

Abstract Ceramide is a bioactive sphingolipid with many associated biological outcomes, yet there is a significant gap in our current understanding of how ceramide mediates these processes. Previously, ceramide has been shown to activate protein phosphatase (PP) 1 and 2A. While continuing this line of work, a late fraction from a Mono-Q column was consistently observed to be activated by ceramide, yet PP1 and PP2A were undetectable in this fraction. Proteomic analysis of this fraction revealed the identity of the phosphatase to be PP2Cγ/PPM1G. This was consistent with our findings that PP2Cγ 1-eluted in a high salt fraction due to its strongly acidic domain, and 2-was insensitive to okadaic acid. Further characterization was performed with PP2Cα, which showed robust activation by C_6-ceramide. Activation was specific for the *erythro* conformation of ceramide and the presence of the acyl chain and hydroxyl group at the first carbon. In order to demonstrate more physiological activation of PP2Cα by ceramide, phospho-p38δ was utilized as substrate. Indeed, PP2Cα induced the dephosphorylation of p38δ only in the presence of C_{16}-ceramide.[JLR] Taken together, these results show that the PP2C family of phosphatases is activated by ceramide, which may have important consequences in mediating the biological effects of ceramide.—Perry, D. M., K. Kitatani, P. Roddy, M. El-Osta, and Y. A. Hannun. **Identification and characterization of protein phosphatase 2C activation by ceramide.** *J. Lipid Res.* **2012.** 53: 1513–1521.

Supplementary key words PP2C • Ser/Thr phosphatases • sphingolipids

Sphingolipids are an enigmatic class of membrane lipids implicated as mediators in several biological processes (1). Ceramide, the central sphingolipid metabolically, has been well studied and is known to be important in apoptosis (2–4), differentiation (5), and inflammation (6, 7).

Despite the vast amount of evidence for the involvement of ceramide in biological processes, a clear mechanistic understanding of how ceramide mediates these effects is not well grasped. However, there are a few emerging biological targets for ceramide, such as protein kinase Cζ (8, 9) and protein phosphatases (PP) 1 and 2A, based on evidence that PP1 and PP2A are activated by ceramide in vitro in a selective and stereospecific manner (10, 11). Biological targets of ceramide activation of these phosphatases include retinoblastoma protein (12), ezrin/radixin/moesin (13, 14), serine/arginine-rich (SR) proteins (15), and p38 (16, 17). However, other serine/threonine (Ser/Thr) phosphatases have not been ruled out as ceramide-activated.

Ser/Thr phoshoprotein phosphatases are comprised of three families: phospho-protein phosphatases (PPPs), metal-dependent phosphatases (PP2C/PPM), and FCP/SCP-like phosphatases (18). PP2C phosphatases can be biochemically distinguished from PPPs by their insensitivity to okadaic acid (OA), a potent inhibitor of PP2A and PP1 (19, 20). The PPP family is comprised of at least 10 catalytic subunits (e.g., PP1Cα), and functional specificity of the PPP family is thought to arise from their ability to interact with numerous regulatory subunits potentially dictating substrate specificity and subcellular localization (21). In contrast, the PP2C family is comprised of at least 16 distinct catalytic genes in humans (22) where an internal regulatory domain may govern substrate specificity and subcellular localization. Despite a lack of sequence homology, there is a similar three-dimensional architecture between PP1 and PP2Cα with a central β-sandwich surrounded by α-helices (23).

In an effort to further characterize the relationship between ceramide and Ser/Thr protein phosphatases, we

Abbreviations: DAG, dipalmitoylglycerol;MBP, myelin basic protein; OA, okadaic acid; PKA, protein kinase A; PP, protein phosphatase; PPP, phospho-protein phosphatase; SR, serine/arginine-rich.
[1] To whom correspondence should be addressed.
  e-mail: Yusuf.Hannun@stonybrookmedicine.edu
[S] The online version of this article (available at http://www.jlr.org) contains supplementary data in the form of a figure.

identified PP2Cγ/PPM1G in a high-salt-eluting fraction from a Mono-Q column as ceramide activated. Further characterization was performed on PP2Cα, the canonical PP2C isoform, showing activation in a stereospecific and selective manner. This work has potential impact on the current understanding of the molecular mechanisms by which ceramide mediates biological outcomes, implicating PP2Cα as a potential target of ceramide signaling.

MATERIALS AND METHODS

Materials

Frozen rat brains were purchased from Pel-Freez Biologicals and A549 cells were from ATCC (Manassas, VA). Protein kinase A (PKA), Myelin basic protein (MBP), and other general chemicals were purchased from Sigma-Aldrich (St. Louis, MO). PP2A and PP1 antibodies for the catalytic subunits were from BD Biosciences (Franklin Lakes, NJ) and Santa Cruz Biotechnology (Santa Cruz, CA), respectively. Active-p38 (phospho) antibody and p38δ antibodies were from Promega (Madison, WI) and R&D Systems (Minneapolis, MN), respectively. Radiolabeled γ-^{32}P-ATP and γ-^{33}P-ATP were from Perkin Elmer (Waltham, MA). C_6-ceramide, dihydro-D-*erythro*-C_{16}-ceramide, D-*erythro*-sphingosine, and D-*erythro*, D-*threo*, L-*erythro*, L-*threo*-C_{16}-ceramides were prepared as described previously (11). C_{18}-ceramide was purchased from Matreya (Pleasant Gap, PA). 1-deoxy-C_{16}-ceramide and dipalmitoyl-glycerol were purchased from Avanti Polar Lipids (Alabaster, AL). Recombinant PP2Cα and p38δ were purchased from ProSpec (East Brunswick, NJ) and Enzo Life Sciences (Farmingdale, NY), respectively.

Fractionation of endogenous phosphatases

Fractionation was performed as described previously (24). In order to identify novel targets of ceramide-activated phosphatases from human sources, A549 lung cancer cells were used, and lysates were used immediately after lysis, compared with previous work which used frozen tissue. Likewise, frozen rat brains were used as a source of starting material to be able to compare with previous work and corroborate findings from A549 cells. Total homogenate from A549 cells (∼10 T150 flasks) or one rat brain was prepared by nitrogen cavitation or passing through a tight-fitting 7 ml Wheaton dounce in lysis buffer containing 50 mM Tris HCl pH 7.4, 1 mM EDTA, 1 mM EGTA, 1 mini-protease inhibitor tablet/10 ml (Roche, EDTA free). Homogenate was cleared by centrifuging at 1,000 *g* for 5 min to remove debris and nuclei. Supernatant was transferred to high-speed tubes and centrifuged at 100,000 *g* for 1 h. All steps were performed on ice or at 4°C.

Soluble lysate was mixed with 5 M NaCl sufficient to bring to a final concentration of 1.5 M NaCl. This was loaded onto a phenyl sepharose column and eluted by decreasing salt concentration to 0 M NaCl. Fractions were tested for phosphatase activity in the absence or presence of C_6-ceramide. Aliquots were also stored for total protein staining or immunoblotting after SDS-PAGE. Fractions eluting from ∼0.5 M through 0 M NaCl were pooled (0.5 ml/fraction), diluted to 50 mM NaCl (50 ml maximum), and then loaded onto a Mono-Q column. This was then eluted by a linear gradient of 50 mM NaCl to 500 mM NaCl. Fractions were then tested for phosphatase activity in the absence or presence of C_6-ceramide and then aliquoted for Coomassie staining and immunoblotting.

Radiolabeling of MBP

MBP was phosphorylated by PKA as described previously (11, 24). Briefly, in two identical reactions, 1 mg MBP was incubated with 200 U PKA, 1 mM ATP, 50 μCi of either ^{32}P γ- or ^{33}P γ-ATP, 10 mM MgCl$_2$, 5 mM DTT, 10 mM βME in a final volume of 500 μl of 50 mM Tris-HCl buffer pH 7.4 for 2 h at 37°C. This was then precipitated with 170 μl TCA (−20°C) on ice for 10-30 min and centrifuged at 15,000 g for 15 min. The supernatant was discarded and the pellet was resuspended in 500 μl of 40 mM Tris-HCl pH 7.4. This was repeated a minimum of three times to effectively remove unincorporated ATP.

Phosphatase activity assays

Phosphatase assays were performed as described previously (11) with minor modifications. Briefly, ceramides and other lipids were dissolved in either ethanol or dodecane-ethanol (2%:98% v/v), which were added to assay buffer (50 mM Tris pH 7.4, 20% glycerol, 1 mM MnCl$_2$, 100 mM NaCl, 1 mM DTT) not exceeding 1% of total volume and preincubated for 5 min at 30°C. For testing activity from FPLC fractions, 2-5 μl of each fraction was incubated for 15 min (phenyl sepharose fractions) or 1 h (Mono-Q fractions) with radiolabeled MBP. For assays with PP2Cα, 5-10 ng of enzyme diluted in assay buffer was incubated in assay buffer for 30 min. Termination of the reaction was achieved by adding 375 μl of cold 55% TCA followed by 275 μl of 0.9 mg/ml BSA. Tubes were capped, vortexed, and incubated for 15 min on ice. Samples were then centrifuged for 30 min at 4°C from which 250 μl of the supernatant was transferred to scintillation vials for measuring radioactivity as a readout of hydrolyzed phosphate. Statistical and kinetic analysis was performed with Prism/GraphPad using nonlinear regression analysis for calculating kinetic paramters.

Protein staining and Western blotting

Fractions were prepared for SDS-PAGE by freezing 0.3 ml at −80°C and subsequent lyophilization overnight. Samples were then resuspended in Laemmli buffer and run on SDS-PAGE for total protein staining or Western blots on nitrocellulose membranes and were incubated overnight with primary antibodies in 5% nonfat milk in PBS/ 0.1% Tween 20. Membranes were washed in PBS/ 0.1% Tween 20 at least three times, incubated with secondary antibodies, washed again, and then developed in ECL chemiluminescence reagent.

Proteomic analysis

Fractions of interest were precipitated by adding 0.9 ml cold 100% acetone to 0.3 ml of each fraction and incubated at −20°C overnight. Samples were centrifuged for 20 min at 45,000 *g* at 4°C. Supernatants were aspirated and then pellets were dried and stored. Acid-dissolved Trypsin Gold was diluted to 20 μg/ml and added to the solubilized pellet and incubated overnight at 37°C for full digestion. The next day, solution was dried in SpeedVac for 2–4 h in preparation to full dryness then resolubilized with 50% acetonitrile/5% at room temperature for MS analysis.

An instrument set of LC/ESI/MS/MS on a linear ion trap mass spectrometer (LTQ, Thermo Finnigan) coupled to an LC Packings nano-LC system was used to analyze the trypsin-digested sample. For reversed phase LC column, a 15-cm × 75 μm C-18 (packed by the Proteomics Core Facility, Medical University of South Carolina) was utilized with a 60 min gradient from 2% acetonitrile, 0.1% formic acid to 60% acetonitrile, 0.1% formic acid at a flow rate of 200 nl/min. A between samples blank was analyzed to limit carryover. In the mass spectrometer, an MS/MS was performed on all ions above an ion count of 1000 using data-dependent analysis. Dynamic exclusion mode was set to exclude ions from MS/MS selection for 3 min after being selected two times in a 30 s window.

The MS/MS data search was performed against mammalian databases using Thermo Finnigan Bioworks 3.3 software. Data search was also set to account for posttranslational modifications of methionine oxidation, carboxamidomethylation of cysteines, and phosphorylation of serine, threonine, and tyrosine.

Dynamic light scattering

Varying concentrations of C_{16}-ceramide were prepared in dodecane/ethanol (2%:98%). This solution was added to activity assay buffer 1:100 (v/v) and analyzed by dynamic light scattering for measurement of particle size using a PDDLS/ Cool Batch 40T/ PD2000 DLS. Settings for measurement included 20°C, 0.01769 P and a refraction of 1.35749.

RESULTS

Identification of PP2Cγ as ceramide-activated

In an attempt to characterize the in vitro activation of Ser/Thr phosphatases by ceramide, the approach developed by Galadari et al. (24) was employed. Soluble lysate from A549 cells or rat brain was fractionated first on a phenyl sepharose hydrophobic exchange column and subsequently on a Mono-Q anionic exchange column. After each column, fractions were tested for phosphatase activity in the presence or absence of C_6-ceramide (ethanol vehicle) using radiolabeled ^{32}Pi-MBP as a substrate. Basal phosphatase activity eluting from the phenyl sepharose column is characterized by a large peak, which generally correlated

with the presence of PP2A according to immunoblots for the catalytic subunit (**Figs. 1** and **2**). As known previously, this activity was stimulated by ceramide roughly two-fold, with particular fractions demonstrating unique sensitivity suggesting specific ceramide sensitive targets, ruling out that this was a general effect. Fractions corresponding to 0.5 M NaCl and later were pooled, diluted, and loaded on a Mono-Q column.

Phosphatase activity derived from A549 eluting from the Mono-Q displayed three peaks of activity (Fig. 1A, right panel. Peak I- fr 72, Peak II- fr 77-78, Peak III- fr 86). The first two peaks correlated with the presence of PP2A by immunoblot, with peak II being clearly activated by ceramide (Fig. 2A, right panel). The two different pools of PP2A are likely a result of specific heterotrimers with unique B subunits (24) conferring differing anionic character. Interestingly, a third peak of low basal activity was observed that lacked PP2A yet was consistently activated by C_6-ceramide. None of the PP1 isoforms (α/β/γ) was detectable by immunoblot (data not shown), suggesting a previously undescribed ceramide-activated phosphatase.

In order to determine whether this phosphatase was in the PPP family, fractions representing peak II and III off the Mono-Q from A549 were analyzed for their sensitivity to OA and ceramide. OA strongly inhibited the PP2A-rich peak II as expected and largely blocked the ceramide activation. In contrast, peak III, which displayed low basal activity, was very sensitive to ceramide stimulation but insensitive
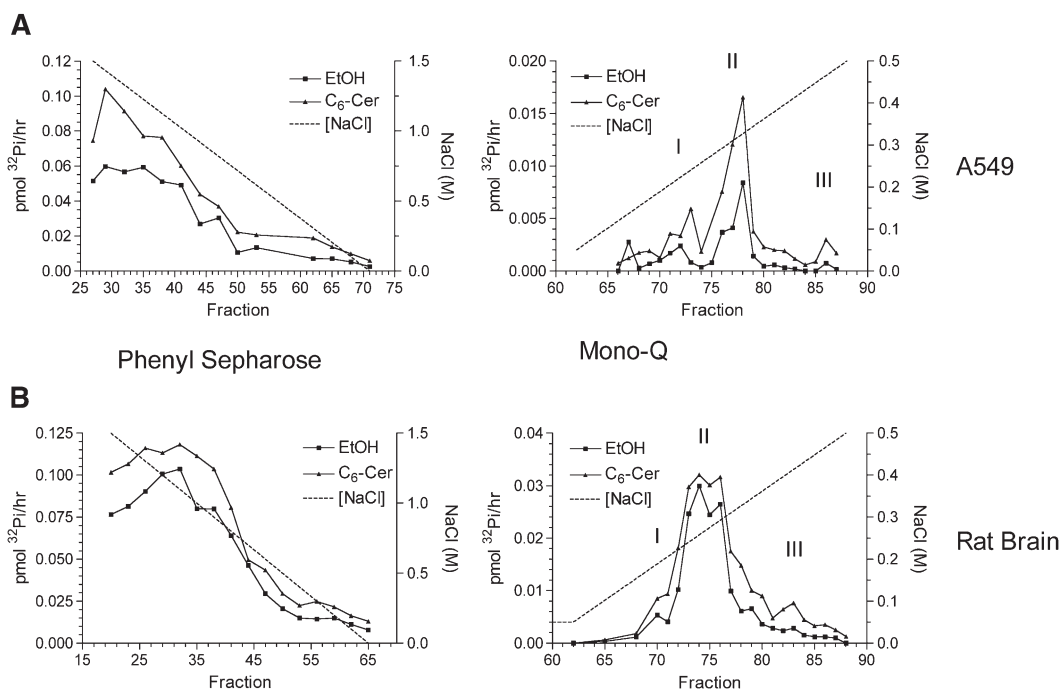

Fig. 1. Ceramide-activation of serine/threonine phosphatase activity in fractions from phenyl sepharose and Mono-Q columns. Soluble lysate from A549 (A) or rat brain (B) was fractionated over phenyl sepharose columns with a gradient from 1.5 M to 0 M NaCl. Fractions were subsequently assayed for phosphatase activity as described in Materials and Methods in the absence or presence of 15 μM C_6-ceramide. Fractions consisting of 0.5 M to 0 M NaCl were pooled and diluted to ∼50 mM NaCl, and then loaded onto a Mono-Q column. Proteins were eluted by a linear gradient from 50 mM NaCl to 500 mM NaCl. Subsequently fractions were assayed in the absence of presence of 15 μM C_6-ceramide. Results are representative of at least three independent experiments.
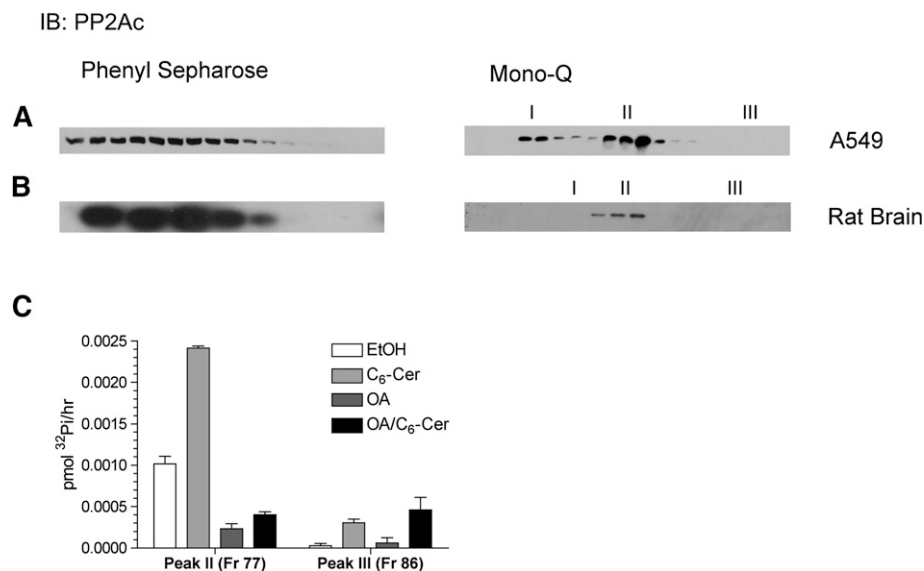
Fig. 2. Characterization of eluting fractions by Western blot and okadaic acid sensitivity. Aliquots of corresponding fractions were prepared for Western blotting for PP2Ac from A549 (A) or rat brain (B). C: Fractions 77 and 86 (peaks II and III) from A549 eluted from the Mono-Q (Fig. 1A) were tested for sensitivity to okadaic acid (100 nM) and C_6-ceramide (15 μM).

to OA in the absence or presence of ceramide (Fig. 2C). These results further argued against the possibility that the identity of the phosphatase in peak III was a previously characterized ceramide-activated protein phosphatase.

Separately, corresponding fractions to peaks I, II, and III were observed from the Mono-Q in rat brain although separation between peaks was less than with A549 lysate (Fig. 1B, right panel). In order to ascertain the identity of the phosphatase in peak III, LC/MS/MS proteomic analysis was performed on fraction 83 from the Mono-Q using rat brain (Fig. 1A, right panel). Two peptide fragments were identified with high confidence matching to PP2Cγ/PPM1G (XC score of 20.27, delta CN of 0.51 and 0.33 for each peptide), which were specific to this fraction, raising the possibility that PP2Cγ was responsible for the ceramide activation of phosphatase activity in peak III. Total protein staining of SDS-PAGE was unable to detect a band in the expected molecular weight range for PP2Cγ in this fraction most likely due to low abundance (data not shown). The PP2C/PPM family of protein phosphatases is metal ion-dependent and insensitive to OA, fitting with the finding that peak III was insensitive to OA. Moreover, PP2Cγ possesses a strongly acidic domain of which it is the only Ser/Thr phosphatase with this domain. This corroborates the finding that peak III corresponds to a high-salt-eluting fraction due to its strong acidic domain yielding a predicted overall pI of 4.36. This is consistent with previous work when it was originally cloned and purified from a Mono-Q column where it also eluted at a similar NaCl concentration (19).

Activation of PP2Cα by short chain and natural ceramides

Further characterization of PP2C activation by ceramide was developed using PP2Cα, the canonical isoform of this family, due to difficulties in expressing active full-length PP2Cγ. To first test whether PP2Cα was also activated by ceramide in vitro, purified recombinant PP2Cα was assayed in the presence of 30 μM C_6-ceramide delivered in ethanol or dodecane/ethanol (2%/98%) as a delivery system because this is the vehicle of choice for long chain ceramides in vitro (**Fig. 3A**, B). Both systems resulted in activation of PP2Cα. Similar results were obtained with other long chain and very long chain ceramides (data not shown). Taken together, the data suggest ceramide was able to strongly activate PP2Cα whether delivered with ethanol or dodecane/ethanol.

A dose response with C_{16}-ceramide was performed on PP2Cα using dodecane/ethanol revealing an EC_{50} of activation of 5.3 μM (Fig. 3C). The lack of linearity with increasing ceramide concentrations on PP2Cα activity suggested a dynamic process was occurring between 4 and 10 μM. To investigate whether this activation was simply a result of particle formation in this range, dynamic light scattering was performed under similar conditions on dodecane/ethanol with increasing C_{16}-ceramide concentrations (supplementary Fig. I). Dodecane/ethanol alone at 1% v/v in activity assay buffer formed particles and upon addition of ceramide, an increase in particle size was observed, which modestly continued for 5 and 10 μM. Due to a lack of a dynamic change in particle size in the range where activation of PP2Cα was seen, it is unlikely that activation by ceramide is simply the result of lipid particle formation.

Effect of ceramide on kinetic parameters of PP2Cα

Next, the effects of ceramide on kinetic parameters of PP2Cα were evaluated. C_{16}-ceramide strongly increased V_{max} while having a minor but notable increase in K_m (**Fig. 4A**, **Table 1**). Overall, there was an increase in k_{cat}/K_m
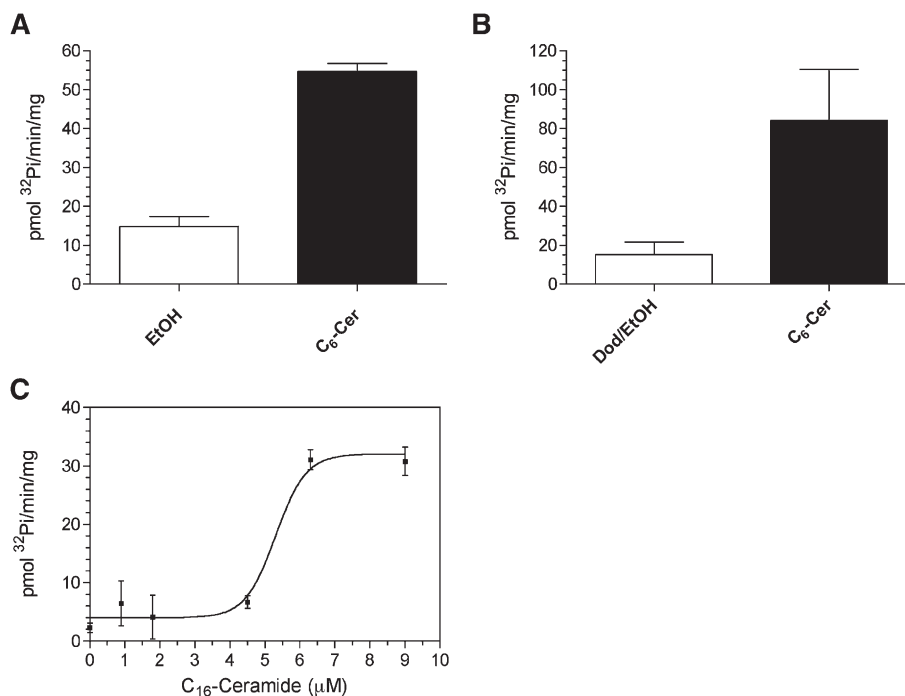
Fig. 3. Activation of PP2Cα by short and long chain ceramides in ethanol and dodecane/ethanol delivery systems. A: Recombinant PP2Cα was assayed in the presence of ethanol, or 30μM C_6-ceramide solubilized in ethanol as described under Materials and Methods. B: PP2Cα was assayed in the presence of dodecane/ethanol or 30 μM C_6-ceramide delivered in dodecane/ethanol. Data represent mean ± SE of four independent experiments. C: PP2Cα was assayed in the presence of increasing concentrations of C_{16}-ceramide delivered in dodecane/ethanol (2%/98%) resulting in an EC_{50} = 5.30 ± 0.33 μM. Result is representative of at least two experiments.

by 3.1-fold. In order to determine whether ceramide regulates the affinity for the metal cofactor, PP2Cα activity was measured at increasing concentrations of $MnCl_2$ in the absence or presence of 10 μM C_{16}-ceramide (Fig. 4B). C_{16}-ceramide resulted in an expected increase in V_{max} with no significant change in K_A for $MnCl_2$ (**Table 2**). This suggests that ceramide may not regulate the affinity of PP2Cα

for its substrate or cofactors but directly activates the enzyme, likely by allosteric change in the conformation of PP2Cα.

Lipid specificity of activation

Ceramide has chiral centers at carbons 2 and 3, yielding four stereoisomers. Evaluation of the enantiomer and
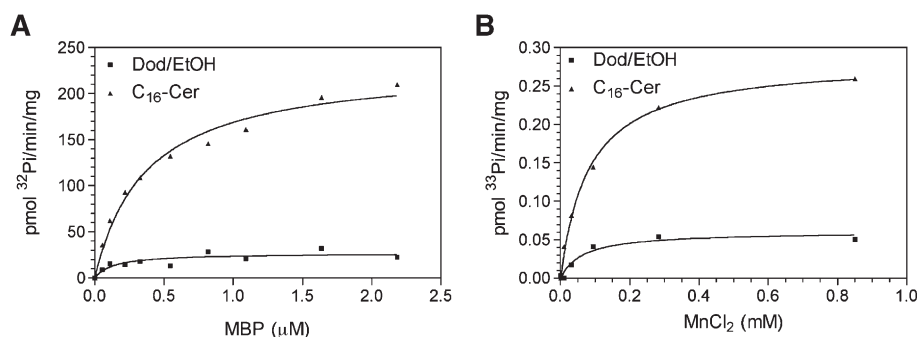

Fig. 4. Effect of C_{16}-ceramide on kinetic parameters of PP2Cα. A: Recombinant PP2Cα was assayed in the presence of dodecane/ethanol or dodecane/ethanol/C_{16}-ceramide (30 μM) at varying concentrations of radiolabeled ^{32}Pi-MBP substrate showing a K_m of 0.133 ± 0.074 μM and 0.368 ± 0.056 μM and a V_{max} of 26.76 ± 3.35 pmol ^{32}Pi/min/mg and 231.2 ± 11.3 pmol ^{32}Pi/min/mg for dodecane/ethanol or C_{16}-ceramide respectively. B: Recombinant PP2Cα was assayed with ^{33}Pi-MBP (1.4 μM) in the presence of dodecane/ethanol or dodecane/ethanol/C_{16}-ceramide (10 μM) at increasing concentrations of $MnCl_2$ showing a K_A of 0.0635 ± 0.0275 mM and 0.0817 ± 0.0073 mM and V_{max} of 0.0600 ± 0.0070 pmol ^{33}Pi/min/mg and 0.2835 ± 0.0073 pmol ^{33}Pi/min/mg for dodecane/ethanol or C_{16}-ceramide, respectively. Data are representative of two experiments.

TABLE 1. Kinetic values of Fig. 4A ± SE

	Dod/EtOH	C_{16}-Ceramide
V_{max} (pmol ^{32}Pi/min/mg)	26.76 ± 3.35	231.2 ± 11.3
K_m (µM)	0.133 ± 0.074	0.368 ± 0.056
V_{max}/K_m	201.20	627.75

diastereomers of D-*erythro*-C_{16}-ceramide demonstrated that the *erythro* conformation (both D-*erythro*- and L-*erythro*) was required for activation of PP2Cα, and the *threo* conformation inhibited activity (**Fig. 5A**).

Other structural variants of ceramide were evaluated to assess the structural requirements for activation of PP2Cα by ceramide. Sphingosine, which lacks the acyl chain, resulted in inhibition of PP2Cα (Fig. 5B). The primary hydroxyl at position 1 proved to be essential for activation due to 1-deoxy-C_{16}-ceramide having no effect on activity (Fig. 5B). Ceramide possesses a unique *trans* double bond at position C4-5, which appeared to not be essential for activation, as dihydro-C_{16}-ceramide was still capable of activation (Fig. 5B). This is distinct from the near lack of activation of PP2A and PP1 by dihydro-ceramides (11).

It has been reported that unsaturated fatty acids are able to activate PP2Cα at high micromolar-to-millimolar concentrations in DMSO (25). In our system, the saturated and unsaturated fatty acids, palmitate and oleate, respectively, both showed inhibition of activity at 10 µM (Fig. 5C) as well as at higher concentrations (data not shown). In order to assess whether this activation is specific to the sphingoid backbone, the glycerolipid, dipalmitoylglycerol (DAG) was compared with C_{16}-ceramide. DAG also displayed activation but was significantly less than C_{16}-ceramide (Fig. 5C). Overall, the results demonstrate stereochemical and structural specificity and selectivity in regulation of PP2C by ceramides demonstrating the headgroup of ceramide to be the critical region for activation.

Ceramide-dependent dephosphorylation of p38δ by PP2Cα

The stress-activated p38 MAP kinase is a well-known in vivo and in vitro substrate for PP2Cα (26, 27). Lack of phosphorylation at Thr180 in the activation loop of p38 was sufficient to completely inactivate p38α (28, 29), implicating this as a possible mechanism for regulation. Previous work from our laboratory has shown that p38 activation is regulated by endogenous ceramide where the p38δ isoform is preferentially targeted (16, 17). Therefore, using phosphorylated p38δ as a phospho-substrate, ceramide activation of PP2Cα was evaluated at varying doses in dodecane/ethanol. PP2Cα alone did not dephosphorylate p38δ noticeably; however, the presence of low micromolar concentrations of ceramide caused a robust

TABLE 2. Kinetic values of Fig. 4B ± SE

	Dod/EtOH	C_{16}-Ceramide
V_{max} (pmol ^{33}Pi/min/mg)	0.0600 ± 0.0070	0.2835 ± 0.0073
K_A (mM)	0.0635 ± 0.0275	0.0817 ± 0.0073
V_{max}/K_A	0.945	3.470

dephosphorylation of p38δ (**Fig. 6A**, B). An additional dose response was performed with C_{16}-ceramide from 100 nM to 1 µM showing effects in the high nanomolar range (Fig. 6C). Additionally, a similar lipid specificity was seen with p38δ as compared with MBP where there was a preference for the *erythro* conformation and sphingoid backbone (Fig. 6D). These results demonstrate that ceramide allows PP2Cα to dephosphorylate p38δ.

DISCUSSION

In this study, PP2C was discovered to be a novel ceramide-activated PP. Using A549 human lung adenocarcinoma cells and rat brain as sources of soluble lysate, a fraction, with relatively low basal activity and devoid of known ceramide-activated protein phosphatases, was activated by C_6-ceramide and later identified by LC/MS/MS from rat brain to be PP2Cγ. In order to further study this interaction, the canonical PP2C isoform, PP2Cα/PPM1A, was used. Both PP2Cγ and PP2Cα were activated under similar conditions by C_6-ceramide delivered in ethanol. C_{16}-ceramide resulted in a robust increase in catalytic activity of PP2Cα, where this activation was stereospecific. Lastly, PP2Cα induced the dephosphorylation of p38δ, a known physiologic substrate of PP2C, only in the presence of C_{16}-ceramide.

This work demonstrates that PP2Cα is robustly and specifically activated by ceramide in vitro. PP2Cα was strongly activated by C_6-ceramide whether delivered in ethanol alone or dodecane/ethanol, demonstrating that dodecane itself was not necessary for activation but possibly enhancing delivery. Moreover, dodecane/ethanol is likely to be more physiological where lipid surfaces or particles are being made; however, the exact nature of this structure is unknown.

Within the sphingoid structure, there was remarkable specificity for ceramide on the activation of PP2Cα. Structure/function studies revealed a requirement for the presence of the acyl chain, primary hydroxyl group, and *erythro* conformation. Moreover, the lack of activation by saturated or unsaturated fatty acids and the diminished activation by DAG compared with ceramide demonstrate the ceramide/PP2Cα interaction to be rather specific. This raises the possibility that there is a unique cavity or pocket in PP2Cα able to sense and respond to ceramide, possessing a hydrophobic pocket with polar residues in the core able to interact with the hydroxyl group and amide of ceramide.

Due to the lack of correlation of activity to particle size, ceramide more likely binds specifically to PP2Cα, provoking an allosteric change rather than nonspecific particle formation resulting in activation. This is further supported by the evidence that *threo* stereoisomers did not activate PP2Cα (Fig. 5A). Standard lipid/protein overlay assays were unsuccessful in detecting binding between ceramide and PP2Cα, an assay that is known not to be well suited for neutral lipids (data not shown). Additionally, conventional methods of delivering lipids, liposomes/micelles, did not result in strong changes in activity (data not shown), suggesting
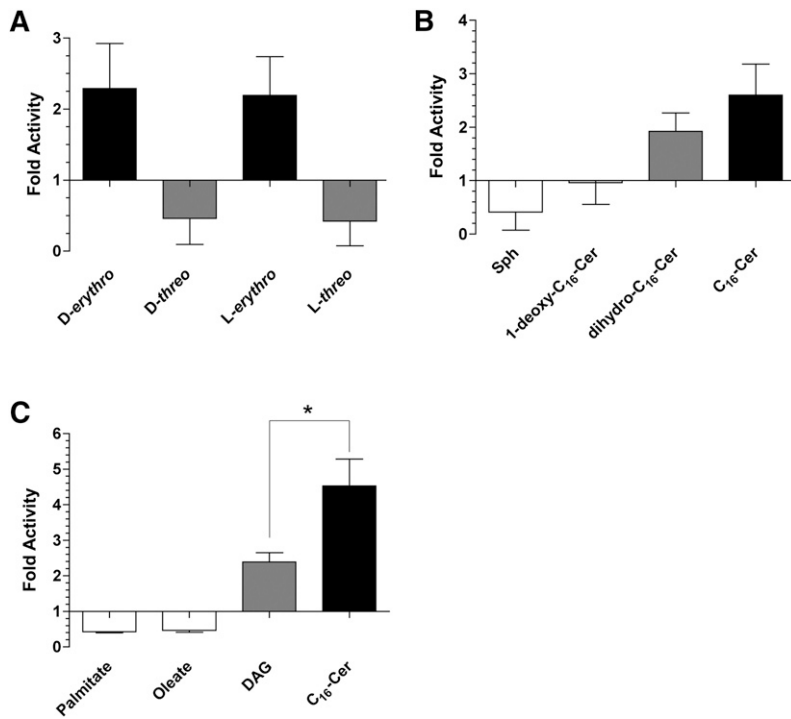
Fig. 5. Lipid specificity of activation of PP2Cα. PP2Cα was assayed in the presence of 10 μM D-*erythro*, D-*threo*, L-*erythro*, or L-*threo*-C$_{16}$-ceramide (A); or 10 μM sphingosine, 1-deoxy-C$_{16}$-ceramide, dihydro-C$_{16}$-ceramide, D-*erythro*-C$_{16}$-ceramide (B); or 10 μM palmitate, oleate, dipalmitoyl-glycerol, or D-*erythro*-C$_{16}$-ceramide (C) as described in Materials and Methods. Data represent mean ± SE of fold change compared with dodecane/ethanol control of at least two independent experiments. Unpaired *t*-test, * $P = 0.023$.

a unique lipid delivery requirement for ceramide to be bioactive in this context such as the requirement for more soluble monomeric ceramide. Taken together, the data indicate the exact nature of the ceramide/PP2Cα interaction

is not understood, and further studies are needed in this regard.

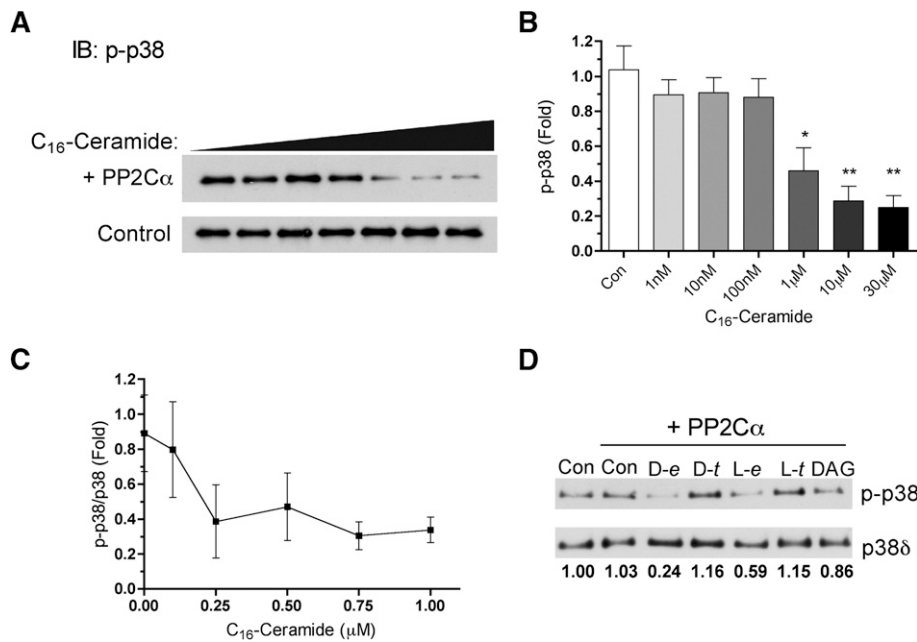Finally, PP2Cα was virtually unable to dephosphorylate p38δ in the absence of ceramide (even at high concentrations

Fig. 6. Ceramide-dependent dephosphorylation of phospho-p38δ. A: PP2Cα activity was measured as described in Materials and Methods using recombinant phospho-p38δ as substrate with increasing concentrations of C$_{16}$-ceramide in dodecane/ethanol (2%/98%). Increasing concentrations of C$_{16}$-ceramide were incubated with recombinant p38δ with or without PP2Cα. B: Phosphorylated p38δ was quantified from the upper panel including PP2Cα using ImageJ software. Data represent mean ± SE of four separate determinations. One-way ANOVA statistical analysis with Bonferroni's post test, * $P < 0.01$, ** $P < 0.001$. C: Concentrations of C$_{16}$-ceramide from 100nM to 1μM were tested on PP2Cα using phospho-p38δ as substrate as described in Materials and Methods. Levels of phospho-p38 and p38δ were quantified and expressed as fold compared with control. D: PP2Cα was assayed using phospho-p38δ as substrate in the presence of 10 μM D-*erythro*, D-*threo*, L-*erythro*, or L-*threo*-C$_{16}$-ceramide or dipalmitoyl-glycerol. The ratio of phospho-p38 to p38δ is expressed as fold change compared with control.

of PP2Cα, which are known to have high activity toward MBP). However, in the presence of low micromolar concentrations of ceramide, there was almost complete dephosphorylation of p38δ. This suggests that with a more physiological phospho-substrate, activation by ceramide may be a direct and robust mechanism for regulation.

Accumulating evidence is emerging that implicates PP2Cα in responses that are known to be regulated by sphingolipids, suggesting cellular connections. First, several lines of work demonstrate that p38 is regulated by the salvage pathway of sphingolipids where ceramide is likely a negative regulator of p38 phosphorylation (16). Inhibition of ceramide-producing enzymes, acid β-glucosidase and ceramide synthase, resulted in enhanced phosphorylation of p38, and conversely, exogenous treatment of cells with C_6-ceramide caused a decrease in p38 phosphorylation induced by phorbol 12-myristate 13-acetate in MCF-7 cells (16, 17). PP2Cα is a key phosphatase of this pathway, known to dephosphorylate Thr180 of p38. This model is consistent with our in vitro data suggesting that ceramide activation of PP2Cα may be an acute mechanism of negative regulation of p38 signaling. Second, SMAD2/3 is regulated by sphingosine-1-phosphate and dihydro-sphingosine-1-phosphate (30). Interestingly, these two lipids have opposite effects on SMAD phosphorylation, which may be mediated through PP2Cα, an essential SMAD2/3 phosphatase. The role of ceramide in this context has not been evaluated where it is possible that ceramide is a negative regulator of SMAD phosphorylation via PP2Cα activation.

The finding that ceramide activates PP2C in addition to PP1/PP2A raises some considerations. As to the target of ceramide, this suggests that the catalytic subunit of the phosphatase is the target based on the monomeric nature of PP2C compared with the more complicated scenario of PP1/PP2A with multiple scaffold and regulatory subunits. Interestingly, despite the lack of sequence of homology between the family of phosphatases, there appears to be a similar structural fold between them, which implies that ceramide may be interacting within this region of the enzyme. However, it is entirely plausible that ceramide has different targets in the context of PP2C versus PP1/PP2A.

In conclusion, this study demonstrates for the first time a connection between ceramide and the OA-insensitive phosphatase family, PP2C. Further study is necessary to probe the physiological significance of this finding in the context of stress signaling.⬛

REFERENCES

1. Hannun, Y. A., and L. M. Obeid. 2008. Principles of bioactive lipid signalling: lessons from sphingolipids. *Nat. Rev. Mol. Cell Biol.* **9:** 139–150.
2. Mullen, T. D., R. W. Jenkins, C. J. Clarke, J. Bielawski, Y. A. Hannun, and L. M. Obeid. 2011. Ceramide synthase-dependent ceramide generation and programmed cell death: involvement of salvage pathway in regulating postmitochondrial events. *J. Biol. Chem.* **286:** 15929–15942.
3. Lin, C. F., C. L. Chen, and Y. S. Lin. 2006. Ceramide in apoptotic signaling and anticancer therapy. *Curr. Med. Chem.* **13:** 1609–1616.
4. Siskind, L. J., T. D. Mullen, K. Romero Rosales, C. J. Clarke, M. J. Hernandez-Corbacho, A. L. Edinger, and L. M. Obeid. 2010. The BCL-2 protein BAK is required for long-chain ceramide generation during apoptosis. *J. Biol. Chem.* **285:** 11818–11826.
5. Kim, M. Y., C. Linardic, L. Obeid, and Y. Hannun. 1991. Identification of sphingomyelin turnover as an effector mechanism for the action of tumor necrosis factor alpha and gamma-interferon. Specific role in cell differentiation. *J. Biol. Chem.* **266:** 484–489.
6. Jenkins, R. W., C. J. Clarke, D. Canals, A. J. Snider, C. R. Gault, L. Heffernan-Stroud, B. X. Wu, F. Simbari, P. Roddy, K. Kitatani, et al. 2011. Regulation of CC ligand 5/RANTES by acid sphingomyelinase and acid ceramidase. *J. Biol. Chem.* **286:** 13292–13303.
7. Nikolova-Karakashian, M., A. Karakashian, and K. Rutkute. 2008. Role of neutral sphingomyelinases in aging and inflammation. *Subcell. Biochem.* **49:** 469–486.
8. Fox, T. E., K. L. Houck, S. M. O'Neill, M. Nagarajan, T. C. Stover, P. T. Pomianowski, O. Unal, J. K. Yun, S. J. Naides, and M. Kester. 2007. Ceramide recruits and activates protein kinase C zeta (PKC zeta) within structured membrane microdomains. *J. Biol. Chem.* **282:** 12450–12457.
9. Wang, G., K. Krishnamurthy, N. S. Umapathy, A. D. Verin, and E. Bieberich. 2009. The carboxyl-terminal domain of atypical protein kinase Czeta binds to ceramide and regulates junction formation in epithelial cells. *J. Biol. Chem.* **284:** 14469–14475.
10. Chalfant, C. E., K. Kishikawa, M. C. Mumby, C. Kamibayashi, A. Bielawska, and Y. A. Hannun. 1999. Long chain ceramides activate protein phosphatase-1 and protein phosphatase-2A. Activation is stereospecific and regulated by phosphatidic acid. *J. Biol. Chem.* **274:** 20313–20317.
11. Chalfant, C. E., Z. Szulc, P. Roddy, A. Bielawska, and Y. A. Hannun. 2004. The structural requirements for ceramide activation of serine-threonine protein phosphatases. *J. Lipid Res.* **45:** 496–506.
12. Kishikawa, K., C. E. Chalfant, D. K. Perry, A. Bielawska, and Y. A. Hannun. 1999. Phosphatidic acid is a potent and selective inhibitor of protein phosphatase 1 and an inhibitor of ceramide-mediated responses. *J. Biol. Chem.* **274:** 21335–21341.
13. Zeidan, Y. H., R. W. Jenkins, and Y. A. Hannun. 2008. Remodeling of cellular cytoskeleton by the acid sphingomyelinase/ceramide pathway. *J. Cell Biol.* **181:** 335–350.
14. Canals, D., R. W. Jenkins, P. Roddy, M. J. Hernandez-Corbacho, L. M. Obeid, and Y. A. Hannun. 2010. Differential effects of ceramide and sphingosine 1-phosphate on ERM phosphorylation: probing sphingolipid signaling at the outer plasma membrane. *J. Biol. Chem.* **285:** 32476–32485.
15. Chalfant, C. E., B. Ogretmen, S. Galadari, B. J. Kroesen, B. J. Pettus, and Y. A. Hannun. 2001. FAS activation induces dephosphorylation of SR proteins; dependence on the de novo generation of ceramide and activation of protein phosphatase 1. *J. Biol. Chem.* **276:** 44848–44855.
16. Kitatani, K., J. Idkowiak-Baldys, J. Bielawski, T. A. Taha, R. W. Jenkins, C. E. Senkal, B. Ogretmen, L. M. Obeid, and Y. A. Hannun. 2006. Protein kinase C-induced activation of a ceramide/protein phosphatase 1 pathway leading to dephosphorylation of p38 MAPK. *J. Biol. Chem.* **281:** 36793–36802.
17. Kitatani, K., K. Sheldon, V. Anelli, R. W. Jenkins, Y. Sun, G. A. Grabowski, L. M. Obeid, and Y. A. Hannun. 2009. Acid beta-glucosidase 1 counteracts p38delta-dependent induction of interleukin-6: possible role for ceramide as an anti-inflammatory lipid. *J. Biol. Chem.* **284:** 12979–12988.
18. Shi, Y. 2009. Serine/threonine phosphatases: mechanism through structure. *Cell.* **139:** 468–484.
19. Travis, S. M., and M. J. Welsh. 1997. PP2C gamma: a human protein phosphatase with a unique acidic domain. *FEBS Lett.* **412:** 415–419.
20. Honkanen, R. E., B. A. Codispoti, K. Tse, A. L. Boynton, and R. E. Honkanan. 1994. Characterization of natural toxins with inhibitory activity against serine/threonine protein phosphatases. *Toxicon.* **32:** 339–350.
21. Cohen, P. T. 2002. Protein phosphatase 1–targeted in many directions. *J. Cell Sci.* **115:** 241–256.

22. Lammers, T., and S. Lavi. 2007. Role of type 2C protein phosphatases in growth regulation and in cellular stress signaling. *Crit. Rev. Biochem. Mol. Biol.* **42:** 437–461.
23. Das, A. K., N. R. Helps, P. T. Cohen, and D. Barford. 1996. Crystal structure of the protein serine/threonine phosphatase 2C at 2.0 A resolution. *EMBO J.* **15:** 6798–6809.
24. Galadari, S., K. Kishikawa, C. Kamibayashi, M. C. Mumby, and Y. A. Hannun. 1998. Purification and characterization of ceramide-activated protein phosphatases. *Biochemistry.* **37:** 11232–11238.
25. Klumpp, S., D. Selke, and J. Hermesmeier. 1998. Protein phosphatase type 2C active at physiological Mg2+: stimulation by unsaturated fatty acids. *FEBS Lett.* **437:** 229–232.
26. Hanada, M., T. Kobayashi, M. Ohnishi, S. Ikeda, H. Wang, K. Katsura, Y. Yanagawa, A. Hiraga, R. Kanamaru, and S. Tamura. 1998. Selective suppression of stress-activated protein kinase pathway by protein phosphatase 2C in mammalian cells. *FEBS Lett.* **437:** 172–176.
27. Takekawa, M., T. Maeda, and H. Saito. 1998. Protein phosphatase 2Calpha inhibits the human stress-responsive p38 and JNK MAPK pathways. *EMBO J.* **17:** 4744–4752.
28. Askari, N., J. Beenstock, O. Livnah, and D. Engelberg. 2009. p38alpha is active in vitro and in vivo when monophosphorylated at threonine 180. *Biochemistry.* **48:** 2497–2504.
29. Zhang, Y. Y., Z. Q. Mei, J. W. Wu, and Z. X. Wang. 2008. Enzymatic activity and substrate specificity of mitogen-activated protein kinase p38alpha in different phosphorylation states. *J. Biol. Chem.* **283:** 26591–26601.
30. Bu, S., B. Kapanadze, T. Hsu, and M. Trojanowska. 2008. Opposite effects of dihydrosphingosine 1-phosphate and sphingosine 1-phosphate on transforming growth factor-beta/Smad signaling are mediated through the PTEN/PPM1A-dependent pathway. *J. Biol. Chem.* **283:** 19593–19602.